



# Climate model spread outweighs glacier model spread in 21st-century drought buffering projections

Lizz Ultee<sup>1,2</sup>, Finn Wimberly<sup>3</sup>, Sloan Coats<sup>4</sup>, Jonathan Mackay<sup>5</sup>, and Erik Holmgren<sup>6</sup>

<sup>1</sup>Cryospheric Sciences Lab, NASA Goddard Space Flight Center, Greenbelt, MD USA

<sup>2</sup>GESTAR-II Cooperative Agreement, Morgan State University, Baltimore, MD, USA

<sup>3</sup>Woods Hole Oceanographic Institution, Woods Hole, MA, USA

<sup>4</sup>Department of Earth Sciences, University of Hawaii at Manoa, Honolulu, HI, USA

<sup>5</sup>Environmental Science Centre, British Geological Survey, Keyworth, UK

<sup>6</sup>Department of Space, Earth and Environment, Chalmers University of Technology, Gothenburg, Sweden

**Correspondence:** Lizz Ultee (elizabeth.ultee@morgan.edu)

**Abstract.** Drought risk is changing as the hydrological cycle responds to anthropogenic climate change. Projections of future drought risk used to inform water management would ideally be conducted at local scale, but local-scale projections demand local data and computational resources that are often not available. As an alternative, global-scale projections of glacier runoff and the hydrological cycle can provide important insights for the local scale, particularly when interpreted carefully. Here, we use an ensemble of latest-generation (CMIP6) climate models to force three different global glacier models, and we examine changes in glacial drought buffering for 75 major river basins in the early, mid-, and late 21st century. Despite differences in absolute glacier runoff simulated by each global glacier model, their glacial drought buffering results are broadly consistent. By contrast, we find that the spread in glacial drought buffering among different climate models is large and likely under-sampled. This work highlights that, for downstream hydrological studies: (1) no one global glacier model is more suitable than another, and (2) analysing a representative ensemble of climate models is imperative. Our findings illustrate that differences in glacier model outputs that appear consequential to glaciologists may be less consequential for downstream impact metrics.

## 1 Introduction

Ongoing anthropogenic climate change has severe consequences for the global water cycle and hydrological hazards (Douville et al., 2021; Caretta et al., 2022). For example, projections from global climate models show robust increases in the severity and frequency of several drought metrics in the coming decades (Cook et al., 2020). Global impact models (Prudhomme et al., 2014) and global hydrological models (Wanders et al., 2015) support similar conclusions. Those projections do not account for changes in parts of the water cycle that are not simulated by those models; for example, glaciers provide substantial runoff to mountain regions, and that cannot be simulated directly in CMIP6-class climate models (Decharme et al., 2019; Lawrence et al., 2019; Ultee et al., 2022, and discussion therein). Although global hydrological models show promise for projecting catchment-scale hydrologic change (Kumar et al., 2022), they include at best a simplistic representation of glacier dynamics



(Wiersma et al., 2022). The regional importance of glacier runoff, and the nonlinear response of glaciers to climate change, demands large-scale glacier-dynamic projections of the impacts of glacier runoff entering major hydrologic systems.

Droughts manifest in response to local environmental conditions that are connected to regional-to-global scale climate. In mountain regions where glacier runoff is significant, projections of drought would ideally come from local-scale hydrological models coupled with glacier evolution models, both driven by regional-to-global scale climate variability and change. There has been progress in coupling glacier evolution models with hydrological models for local- to regional-scale analyses, generally by driving a hydrological model with pre-generated glacier runoff for a short, contemporary period (Naz et al., 2014; Mackay et al., 2018, 2019; Wiersma et al., 2022; Pesci et al., 2023; Hanus et al., 2024). However, it is not yet possible to produce multidecadal projections of glacio-hydrological dynamic evolution for all glacier-dependent basins. Coupled hydrological models are computationally expensive and rely on tens of parameters that are poorly constrained by observations (van Tiel et al., 2020b; Somers and McKenzie, 2020; Hanus et al., 2024). Moreover, the computational, analytical, and observational resources necessary to develop these analyses are not equitably distributed, and often unavailable in the settings that most need it (Stein et al., 2024). In the many basins where fine-scale coupled glacio-hydrological simulations are not yet possible, we can analyse the drought buffering role of glaciers — excluding interactions with snowpack or groundwater — from the combined output of global climate models and glacier models.

Most glacierized river basins contain tens, hundreds, or thousands of individual glaciers, many of which lack in situ ice thickness or runoff observations (Salzmann et al., 2014). Projecting future runoff for such basins requires a model that can efficiently simulate multiple glaciers, at multi-decadal time scales, using only remote sensing or large-scale reanalysis data as inputs. Several such models, known as global glacier evolution models (hereafter “glacier models”), are now available (Huss and Hock, 2015; Maussion et al., 2019; Hock et al., 2019; Rounce et al., 2020). Regional-to global-scale simulations from these models predict dramatic loss of present-day glacier mass during the 21st century, with an initial increase and subsequent decrease in annual glacier runoff (Huss and Hock, 2018; Immerzeel et al., 2020; Wimberly et al., 2025; Schuster et al., 2025).

Previous projections with one glacier model forced by previous-generation (CMIP5) climate model simulations found that glacial drought buffering on the Standardized Precipitation Evapotranspiration Index (SPEI) continued through the end of the 21st century in almost all major river basins worldwide (Ultee et al., 2022). The availability of updated projections from climate models (“CMIP6”, Eyring et al., 2016) and large apparent discrepancies in runoff projections from different glacier models (Wimberly et al., 2025) motivate an evaluation of the sensitivity of glacial drought buffering projections to these changes. Here, we expand the glacial drought buffering analysis of Ultee et al. (2022) to include three different glacier models, forced by a common ensemble of simulations from 11 CMIP6 climate models, for 75 glacierized river basins worldwide.

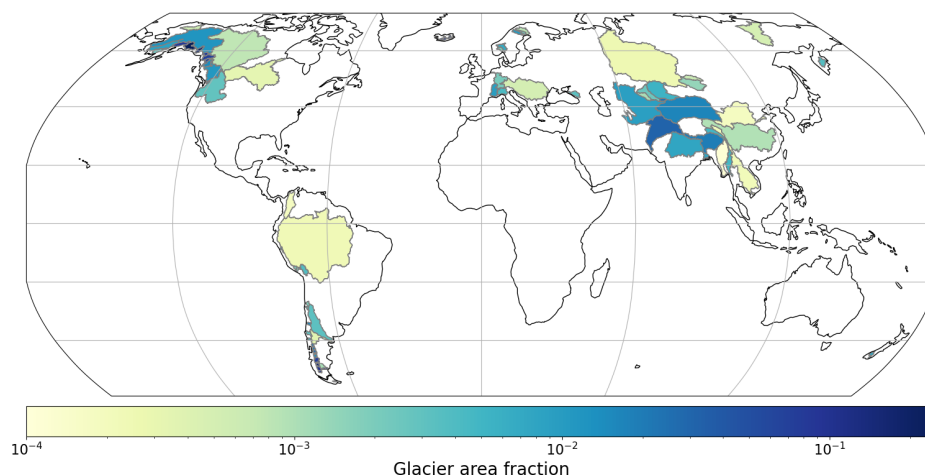


**Figure 1.** Map of river basins included in this analysis: 75 large river basins, each at least 3000 km<sup>2</sup> in area, with glacier cover of at least 30 km<sup>2</sup> in the Randolph Glacier Inventory v6 (RGI Consortium, 2017). Basin outlines are from the Global Runoff Data Centre (Global Runoff Data Centre, 2020), here colored according to their initial glacier area fraction  $A_g/A_{basin}$ . See Appendix for regional maps with basin names.

## 50 2 Methods

### 2.1 Study areas

Our analysis focuses on the world's 75 large river basins (> 3000 km<sup>2</sup>) that have considerable glacier cover (> 30 km<sup>2</sup>), consistent with Wimberly et al. (2025). They are shown in global map view in Figure 1, and in regional maps with basin names in Figs. A1-A5.

55 We analyse model spread in drought buffering and its forcing variables for each basin. The basins appear as markers with whiskers in Figure 2, plotted according to their glacier area fraction. In Figure 3, each panel shows a single basin with its name, organized by region (labelled at the right side of the figure). Figures 4-5 present global climate model ensemble range and mean, with the basins in the same order and labelled by region. Figures B1 and B2 show time series of the forcing variables for each basin, with the same organization as Figure 3. We summarize aggregate results below; where we use specific basins  
 60 as examples, we indicate the basin name, region, and its (row, column) location on the figure when applicable.

### 2.2 Global glacier runoff projections

We analyse a set of projections generated by three glacier models: the Global Glacier Evolution Model (“GloGEM”; Huss and Hock, 2015, 2018), the Python Glacier Evolution model (“PyGEM”; Rounce et al., 2020), and the Open Global Glacier Model (“OGGM”; Maussion et al., 2019, 2023). The projections are forced by a common set of a single continuous historical  
 65 (2000-2014) and Shared Socioeconomic Pathway (SSP) 2-4.5 (2015-2100) simulation from 11 CMIP6 global climate models



(hereafter GCMs). The forcing ensemble is consistent with standard, publicly archived glacier projections (Compagno et al., 2022; Rounce et al., 2023; Schuster et al., 2023b; Zekollari et al., 2024; Wimberly et al., 2025). The three glacier models provide glacier-by-glacier projections of glacier volume and fixed-gauge water runoff, with monthly resolution, for the period 2000-2100. We analyse the runoff output in detail in Wimberly et al. (2025).

## 70 2.3 Drought buffering

Changes in glacier runoff do not translate directly to changes in downstream water supply. Among the many fates possible after leaving the glacial environment, runoff may flow rapidly along surface channels, seep slowly through subsurface pathways, or be lost to evapotranspiration, altering the timing and quantity of water availability. For that reason we use a metric of downstream water supply that accounts for catchment hydrological processes, including potential changes with future climate change: the Standardized Precipitation-Evapotranspiration Index (SPEI).

### 2.3.1 SPEI<sub>G</sub>

We compute two versions of the SPEI following the methods described in Ultee et al. (2022). We do not analyse either version of SPEI in isolation; our work is not intended to produce a projection of actual drought frequency or severity. Rather, we analyse “drought buffering” as the difference between SPEI with no dynamic glacier runoff (SPEI<sub>N</sub>) and SPEI that accounts for glacier runoff (SPEI<sub>G</sub>). We are most interested in how the buffering effect may change over time.

The “no glaciers” SPEI<sub>N</sub> uses only GCM output without accounting for glacier runoff. For each month between 1900-2100, we compute a water balance  $D = P - PET$ , where  $P$  is precipitation and  $PET$  is potential evapotranspiration. The PET computation uses a Penman-Monteith method modified to allow time-varying stomatal conductance in response to CO<sub>2</sub> forcing (Yang et al., 2019). We integrate the  $D$  series over a 3-month scale, such that the integrated value at each time step is the sum of that month and the two previous, which focuses our analysis on streamflow drought (e.g. López-Moreno et al., 2013; Ultee et al., 2022, Appendix B). We then standardize all  $D$  values against those in a climatological reference period (1900-1979), using a nonparametric rank standardization such that unusually high  $D$  values are assigned to SPEI values  $\geq 1$  and unusually low values to SPEI  $\leq -1$  without assuming an underlying distribution shape (Farahmand and AghaKouchak, 2015). The “with glaciers” SPEI<sub>G</sub> is analogous, but replaces the moisture source term  $P$  in the water balance with an area-weighted sum of precipitation over ice-free areas and glacial runoff (including both ice melt and liquid precipitation) over initially glacierized areas:

$$\tilde{P} = \frac{A - A_g}{A} P + R \quad (1)$$

where  $\tilde{P}$  is the modified moisture source,  $A$  is total basin area,  $A_g$  is initially glacierized area of the basin, and  $R$  is glacial runoff from all glaciers that drain into the basin. The climatological reference period does not include glacier runoff, which makes an absolute comparison between SPEI<sub>G</sub> and SPEI<sub>N</sub> less meaningful; for that reason, we focus on changes in buffering over time.



Following standard operational practice (e.g. Danandeh Mehr and Vaheddoost, 2020), we identify a “drought” as any period when the SPEI reaches a threshold value of -1 for at least one month. The “severity” of a given drought is the cumulative sum of SPEI over the period for which SPEI is continuously negative surrounding the month(s) that reach the drought threshold.

100 For each of the river basins studied here, we report the average severity of all droughts within a given time period.

We analyse SPEI data for the 21st century, 2000-2100, in three 21-year periods. The “Early century” is 2000-2020, “Mid-century” 2040-2060, and “Late century” 2080-2100. The glacial drought buffering in the “Early century” is considered a baseline for each basin, by which we assess future changes in buffering. For example, if the difference in severity between  $SPEI_N$  and  $SPEI_G$  is positive during the Early century and becomes more positive in the Late century, then buffering is projected to increase.

105

## 2.4 Model spread

The sources of uncertainty in the drought buffering metric we analyse include structural uncertainty among GCMs, structural uncertainty among glacier models, parameter uncertainty in glacier models, uncertain future climate scenarios, and internal climate variability. The impacts of these uncertainties vary regionally and are most effectively quantified at regional scale (e.g. Aguayo et al., 2024). For this global analysis, we focus on comparing the spread in glacial buffering of drought severity, and changes in that buffering over time, across GCMs and across glacier models. This comparison will not fully quantify the known sources of uncertainty described previously, but it can inform glaciologists and practitioners as to the relative dependence of downstream impact metrics on choice of glacier model.

110

We calculate drought buffering statistics for each glacier model-GCM pair. We then analyse the results for individual glacier models, showing the spread from the GCM forcing ensemble for that glacier model (whiskers in Figure 2b and 3). The “GCM spread” is the difference between the ensemble members ( $N = 11$ ) predicting highest buffering versus lowest buffering for a given glacier model, basin, and period. The “glacier model spread” is the difference between the glacier models ( $N = 3$ ) predicting highest versus lowest multi-GCM mean buffering for a given basin and period. We report the ratio of GCM spread to glacier model spread in Figure 3.

115

As noted in Wimberly et al. (2025), the available glacier runoff data represents the entire population of glacier models available for global runoff simulations, but only a small sample of the GCM forcing realizations from the CMIP6 archive. One of the GCMs included in the Wimberly et al. (2025) ensemble lacks the secondary output variables necessary for calculating SPEI — surface temperature, surface pressure, specific humidity at the surface, and surface net radiation — which means it cannot be included in our analysis. To contextualize the inter-GCM spread not sampled in the current archive of glacier runoff simulations, we compare the precipitation and temperature from our standard forcing ensemble against a larger ensemble of all CMIP6 simulations that include the variables and scenarios necessary for our analysis (Figures 4-5 and B1-B2 below; CMIP6 ensemble from Eyring et al., 2016). This wider ensemble (112 simulations from 24 distinct GCMs) includes spread from both structural uncertainty and internal variability, which we do not attempt to separate.

120



### 3 Results

130 Glacier drought buffering as measured in SPEI is projected to continue through the 21st century. This result is robust to differences in GCM forcing, choice of glacier model, and choice of baseline periods, all of which differ between our study and Ultee et al. (2022). However, we find that GCM spread — arising from natural climate variability as well as differences in climate model construction — has not been well sampled in current glacier projections.

#### 3.1 Magnitude of glacial drought buffering correlates with glacier area fraction

135 Glacial drought buffering is strongest in moderately glacierized basins. The strength of buffering, expressed in terms of reduced number of droughts as well as reduced drought severity, increases as glacier area fraction  $\left(\frac{A_g}{A_{basin}}\right)$  increases, with a decrease for the most heavily glacierized basins (Figure 2a). This result is consistent with glacial drought buffering computed for a single glacier model by Ultee et al. (2022), as well as with theoretical understanding of hydrological trade-offs as basin glacier cover increases (Chen and Ohmura, 1990; van Tiel et al., 2020a).

#### 140 3.2 Change in glacial drought buffering over time consistent among glacier models

Glacial buffering of drought severity generally persists or increases through the end of the 21st century. About 45% (102 cases) of all glacier model-basin pairs (3 glacier models x 75 basins) show no change in GCM ensemble mean buffering between the Early and Late century, and a further 38% show increased buffering (85 cases; Figure 2b). The more heavily glacierized basins tend to show larger increases in GCM ensemble mean buffering, though with more inter-GCM spread.

145 Although there are differences among glacier models in the magnitude of projected changes — buffering of drought severity shown on the vertical axes in Figures 2-3 — the pattern over time for a given basin is similar across glacier models. For example, buffering in the Aral Sea basin (Asia; row 2, column 7 of Figure 3) is positive in the Early century, increases in the Mid century, and remains high through the Late century for GloGEM (green markers), PyGEM (purple markers), and OGGM (blue markers). In other basins, such as the Indigirka (Asia; row 1, column 3), buffering is weak but does not decrease through  
 150 the end of the century, irrespective of choice of glacier model. There are a handful of basins where buffering does decrease later in the century for all three glacier models, e.g., the Kuban (Europe; row 10, column 7). Among the 225 cases shown (75 basins x 3 time periods) there are only 7 for which glacier models disagree on the sign of change. In all cases, GCM ensemble mean buffering for each glacier model falls within the inter-GCM spread of the other two glacier models. We therefore conclude that the qualitative patterns of glacial drought buffering are robust to choice of glacier model.

#### 155 3.3 Inter-GCM spread in glacial drought buffering is substantial and under-sampled

Although ensemble mean glacial drought buffering is consistent across glacier models, there is considerable inter-GCM spread (whiskers in Figures 2-3). Inter-GCM spread always exceeds inter-glacier-model spread. For example, comparing end-of-century buffering, inter-GCM spread exceeds inter-glacier-model spread by factors ranging from 1.7 (Majes basin, South America; row 5, column 7 of Figure 3) to 133 (Magdalena basin, South America; row 4, column 4). In most basins (55 of 75),

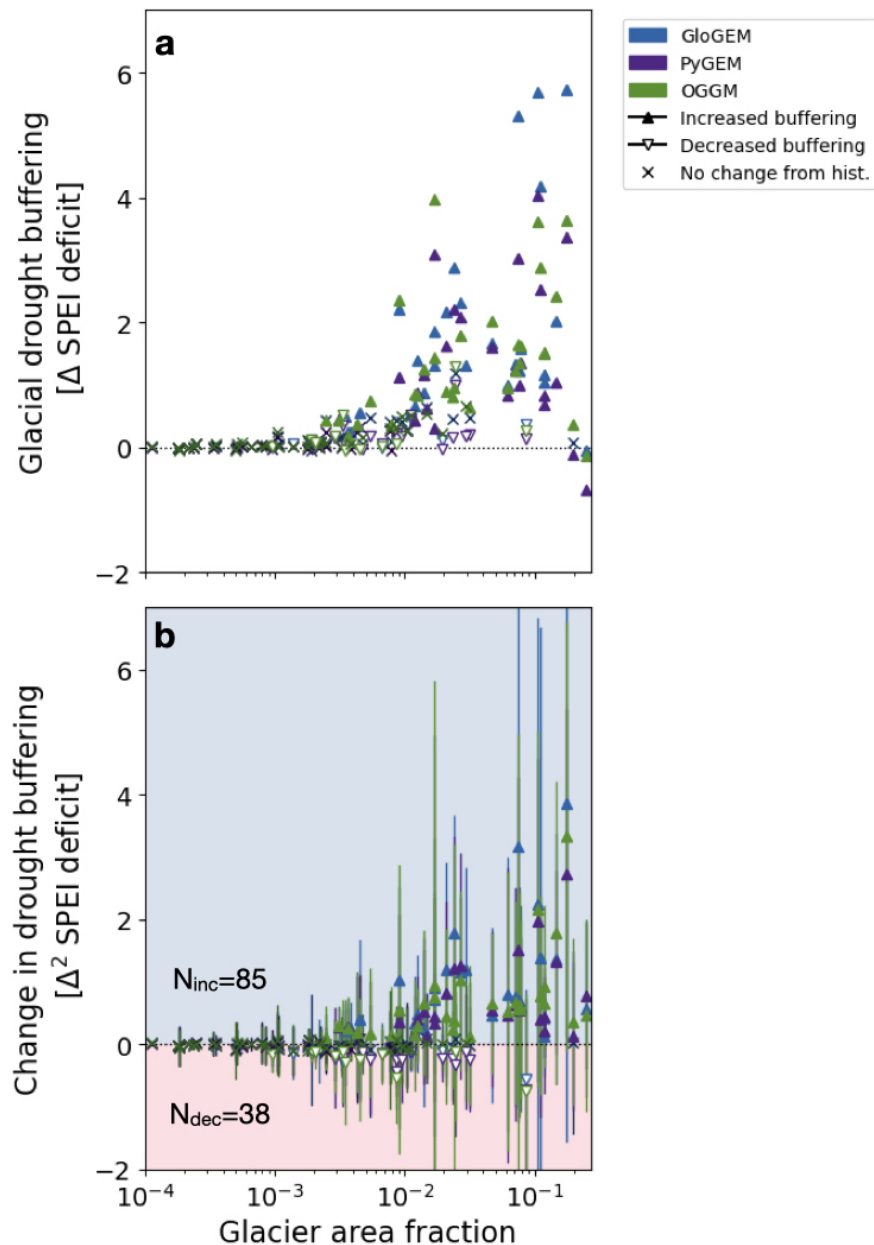


**Figure 2.** (a) Late century (2081-2100) glacial buffering of drought severity, and (b) change in buffering between the Early (2000-2020) and Late century. Both panels show results for the ensemble of 11 GCMs, forcing each glacier model studied here: PyGEM in purple, GloGEM in green, and OGGM in blue. Upward filled carets indicate buffering increased from the baseline; downward open carets indicate buffering decreased; X markers indicate that the change in buffering is within  $\pm 0.1$  SPEI. Panel (a) shows only the ensemble mean, for readability. Panel (b) shows the ensemble mean change in buffering, with full 11-GCM spread in whiskers. Annotations on panel (b) give the number of basin-glacier model pairs with increased ( $N_{inc}$ ) or decreased ( $N_{dec}$ ) buffering; the total number of basin-glacier model pairs is  $75 \times 3 = 225$ .



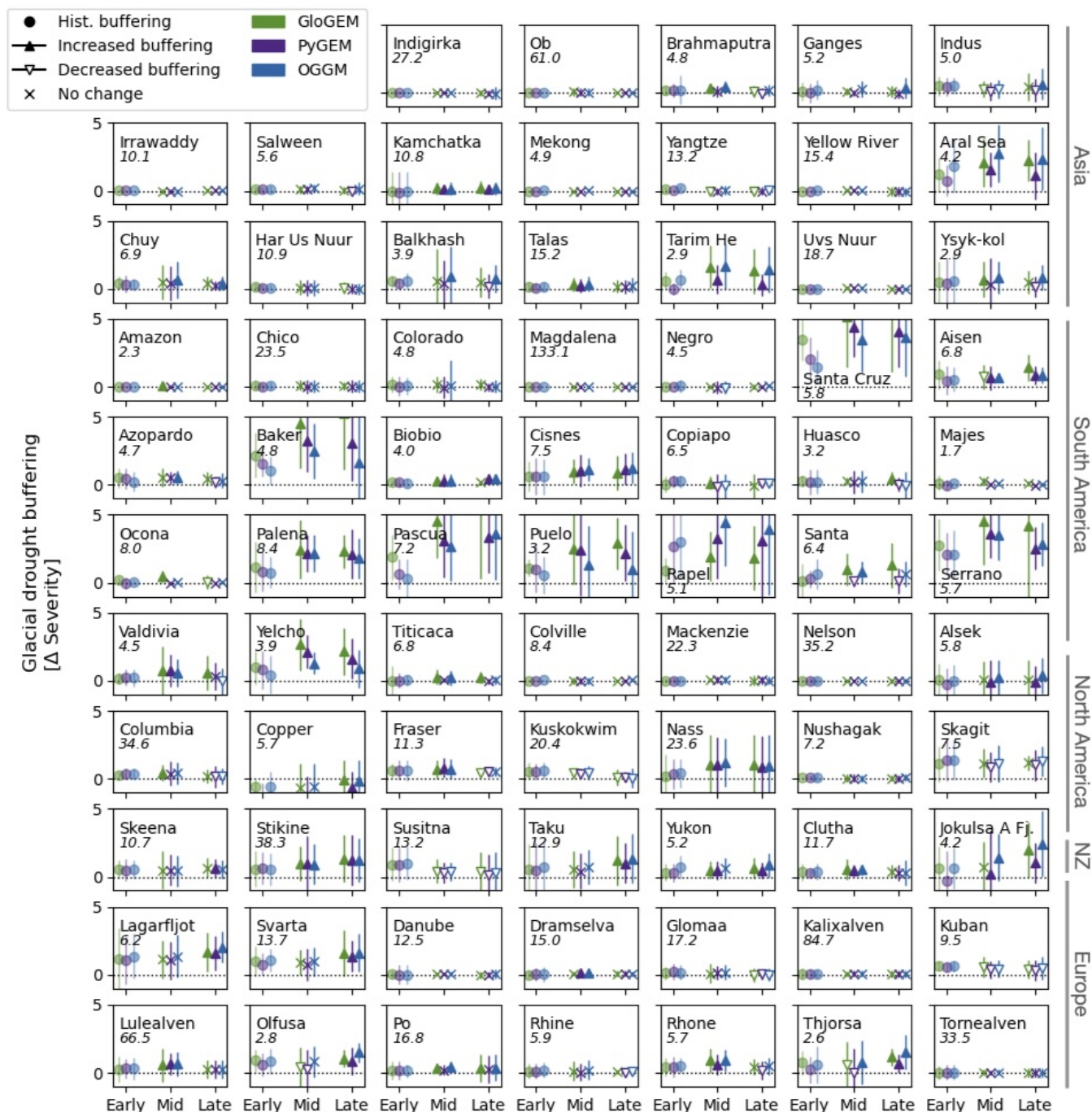


**Figure 3.** 21st-century glacial drought buffering, expressed as difference in drought severity, for three periods: Early (2000-2020), Mid (2040-2060), and Late century (2080-2100). Colors indicate results per glacier model; markers indicate if the GCM ensemble mean buffering increases (upward filled triangles), decreases (downward open triangles), or remains unchanged (x) relative to the historical baseline (circles in Early century). Whiskers give inter-GCM spread. Italic text gives ratio of inter-GCM to inter-glacier-model spread at Late century.





inter-GCM spread is at least five times the spread across glacier models. This is true not only in basins with strong buffering such as the Rapel (South America; row 6, column 5), but also moderate buffering cases such as the Indus (Asia; row 1, column 7) and Fraser (North America; row 8, column 3), and weak buffering cases such as the Danube (Europe; row 10, column 3). Ensemble members tend to agree in sign with the GCM ensemble mean change, but there are several cases in which one or more GCMs projects a change over time of opposite sign to the GCM ensemble mean. Those cases are legible in Figure 2b, where some GCM ensemble members show decreasing buffering (whiskers ending at negative y-axis values) despite a positive GCM ensemble mean change (markers with positive y-axis values).

The 11-member GCM ensemble we analyse here, and which has been used as the standard forcing for glacier models, under-samples uncertainty in the CMIP6 archive. If the glacier-forcing ensemble were representative of the larger CMIP6 archive (Eyring et al., 2016), we would expect the precipitation and temperature series of the 11 members to be well dispersed among those of a larger ensemble. We would also expect the mean values of the smaller ensemble to be close to the mean values of the larger ensemble for most basins. Instead, in comparison to the larger, 112-member CMIP6 ensemble, 21st-century precipitation and temperature projections from the glacier-forcing ensemble sample a smaller range and their means are biased low (Figures 4-5, B1-B2). For example, the glacier forcing ensemble members shown in Figure 4a sample a much more limited range of precipitation change (y-axis values) than the CMIP6 ensemble members shown in Figure 4b. The mean change at end of century is consistently larger amplitude in the CMIP6 ensemble than in the glacier forcing ensemble for both precipitation (Figure 4c) and temperature (Figure 5c). Without generating glacier runoff projections for a more complete sampling of the CMIP6 archive — a computational demand beyond what has been attempted by the glacier modelling community thus far — the uncertainty from GCMs in projections of future glacial runoff and drought buffering remains poorly quantified. Understanding the sources of GCM ensemble spread, and how it differs regionally, for both the standard glacier-forcing ensemble and the CMIP6 archive, merits attention in more detailed studies.

Our results demonstrate conclusively that inter-GCM spread outweighs inter-glacier-model spread in glacial drought buffering projections. More generally, although we have not fully sampled the relevant sources of uncertainty, our findings suggest that uncertainty in climate forcing from GCMs is more important than uncertainty in glacier model physics for hydrological projections in glacierized river basins.

## 4 Discussion

Glacier models use different approaches to simulate glacier processes, so we should expect some resulting differences in their runoff outputs. For example, differences in the approach to calibration, climate-forcing downscaling, and initialization can produce large differences in simulated glacier mass and runoff (Marzeion et al., 2020; Schuster et al., 2023a; Aguayo et al., 2024; Wimberly et al., 2025). This is in fact desirable, allowing the glacier modelling community to sample structural uncertainty — because our models are always an imperfect simplification of the physical world, and we want to capture the range of possibilities — so we should not strive to find one “best-performing” glacier model for every application. Indeed, any

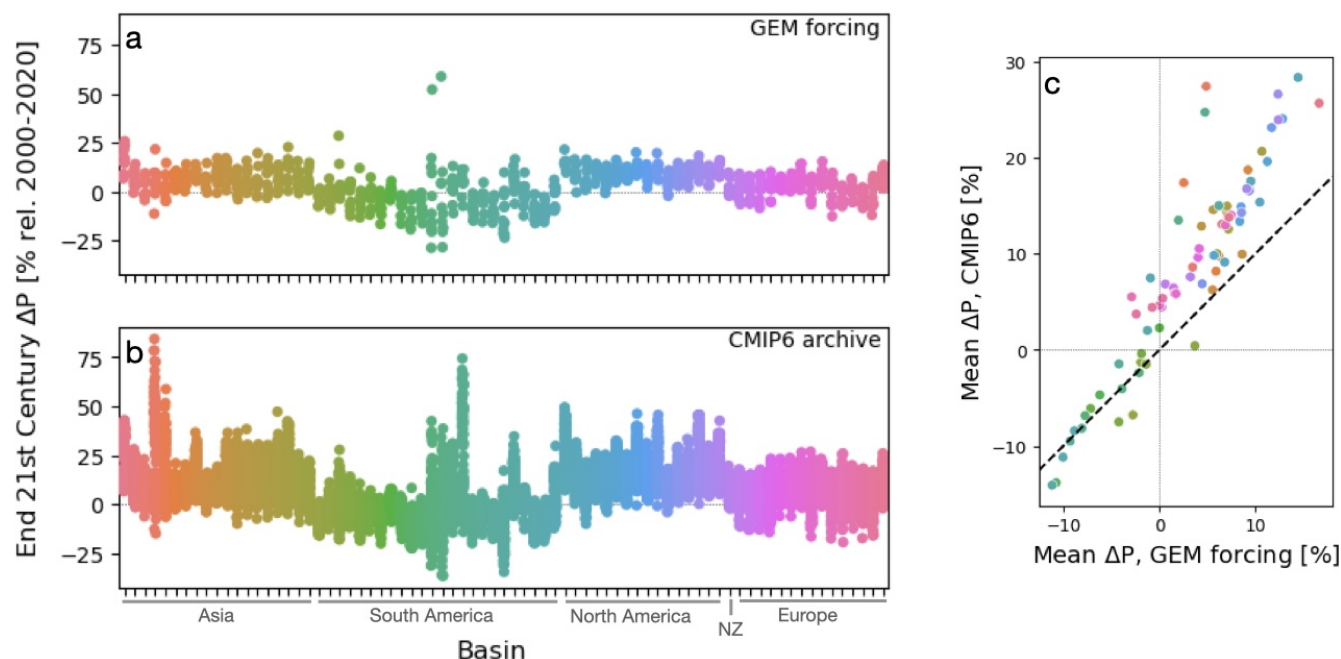


**Figure 4.** Spread in end-of-century (2081-2100) percent change in total basin precipitation for (a) the 11 members of the glacier model forcing ensemble and (b) the 112 members of the CMIP6 archive with data sufficient for SPEI. Panel (c) compares the ensemble means of the same variable, with the glacier model forcing ensemble mean on the x-axis and the CMIP6 ensemble mean on the y-axis; dashed black line shows 1:1 correspondence. Results are colored by basin and shown in the same basin order as other figures; time series for each basin are shown in Figure B1.

evaluation of “performance” depends on context and the intended use case (O’Loughlin, 2024). Our objective here is rather to provide interpretive guidance for use cases that may not otherwise characterize inter-glacier-model uncertainty.

The magnitude of glacial drought buffering correlates with basin glacier coverage in all three glacier models (Figure 2). The nonlinear relationship of glacier coverage and basin streamflow is well theorized (Chen and Ohmura, 1990; Fleming and Clarke, 2005; van Tiel et al., 2020a); it is reassuring that glacier models reproduce the theoretical expectation regardless of differences in process parametrizations. This finding implies that any of the three glacier models chosen would be appropriate for regional-scale analysis. Hence, in a regional-scale runoff study conducted with limited computational resources, it may not be necessary to sample an ensemble of different glacier models.

The qualitative trends in glacial drought buffering over time also do not depend on the choice of glacier model (Figure 3). Despite differences among glacier models in terms of absolute runoff projections (i.e. physical units), the projected annual and seasonal runoff expressed as percent changes are generally similar (Wimberly et al., 2025). The rank standardization used to compute a nonparametric SPEI (Farahmand and AghaKouchak, 2015; Ultee et al., 2022) will likely translate similar percent changes in runoff to similar SPEI changes, other inputs being equal. This renders our findings unsurprising from a statistical

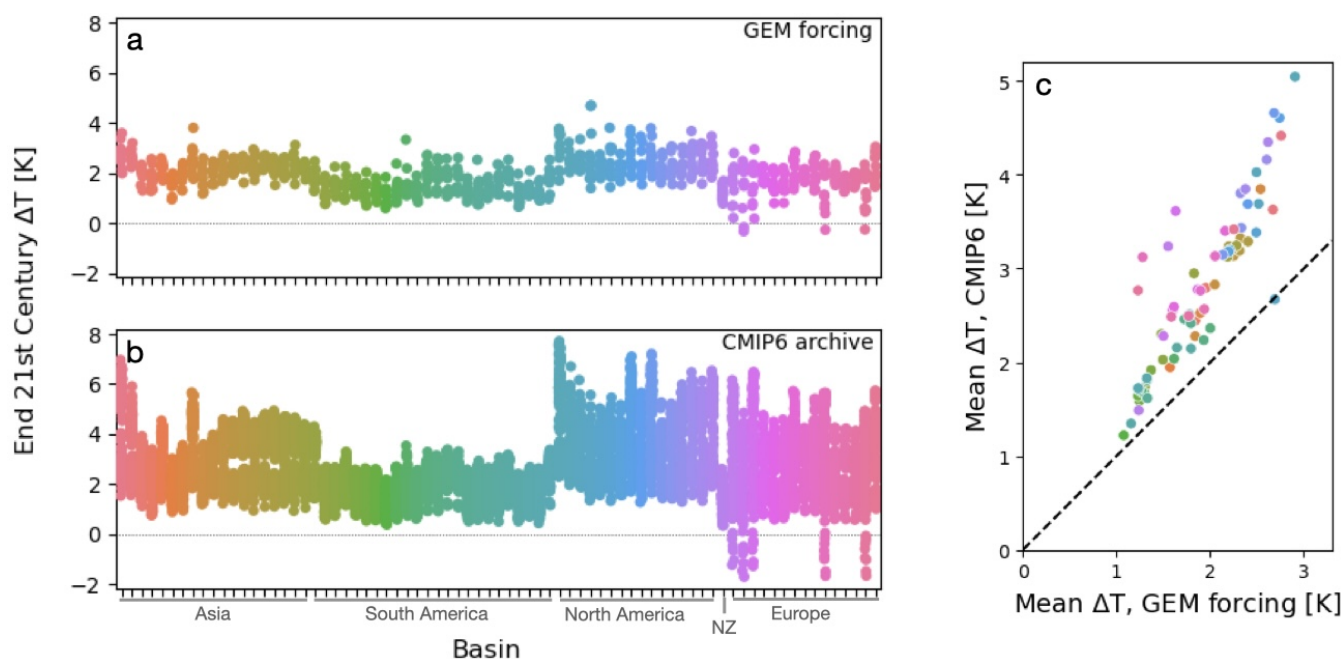


**Figure 5.** Spread in end-of-century (2081-2100) basin-averaged temperature anomaly for (a) the 11 members of the glacier model forcing ensemble and (b) the 112 members of the CMIP6 archive with data sufficient for SPEI. Panel (c) compares the ensemble means of the same variable, with the glacier model forcing ensemble mean on the x-axis and the CMIP6 ensemble mean on the y-axis; dashed black line shows 1:1 correspondence. Results are colored by basin and shown in the same basin order as other figures; time series for each basin are shown in Figure B2.

perspective. Nevertheless, our results demonstrate explicitly that differences in glacier model outputs (here runoff) that appear large to glaciologists may be relatively less important for downstream impact metrics (here the drought index).

Inter-GCM spread emerges as a larger source of uncertainty than inter-glacier-model spread in this analysis. The ensemble of GCM simulations in our results was chosen to be consistent with previous glacier modelling efforts (Compagno et al., 2022; Rounce et al., 2023; Schuster et al., 2023b; Zekollari et al., 2024; Wimberly et al., 2025), which selected ensemble members agnostically, and it is not representative of the full CMIP6 ensemble spread in the 75 river basins we study. We do not attempt to separate GCM structural uncertainty from internal variability, and it is likely that the ensemble of climate forcing undersamples both. For instance, internal climate variability may be large in basins affected by modes of climate variability such as the El Niño-Southern Oscillation (Deser et al., 2020). Furthermore, choosing 11 of over 35 available CMIP6 GCMs is unlikely to fully quantify structural uncertainty. The under-sampling of both structural uncertainty and internal climate variability is apparent in the limited spread of precipitation and temperature projections from the glacier-forcing ensemble compared with a 112-member CMIP6 ensemble (Figures 4-5 and B1-B2). Finally, our drought buffering analysis includes only a single climate scenario. Thus, although our previous analyses indicate that scenario uncertainty may be comparable in magnitude to other GCM uncertainties (Ultee et al., 2022; Wimberly et al., 2025), we have not quantified it here. Fully quantifying the uncertainty



from internal variability, scenario uncertainty, and structural uncertainty at the scale of the river basins of interest should be a high priority for future studies.

Aside from GCM and glacier model-related uncertainty, the definition of “drought” is also a consequential source of uncertainty in future projections (Satoh et al., 2021; Caretta et al., 2022). The SPEI, like other drought indices, is a statistical metric that does not account for physical processes other than those explicit in its input data (Scheff et al., 2022). Our results are therefore not to be interpreted as a definitive projection of future drought or glacial drought buffering. Most notably for the mountain basins we describe here, SPEI does not explicitly account for changing snowpack, interactions with groundwater stores, or human interventions in regional water flow (Van Loon et al., 2016). Local- to regional-scale drought assessments should apply more detailed modelling frameworks and monitoring data capable of quantifying regionally important dynamics.

Although the three glacier models we analyse are nearly interchangeable in terms of quantifying drought buffering, there are inter-glacier model differences that may make one more suitable than another for specific regional applications. For example, PyGEM is the only one that includes explicit treatment of debris cover on glaciers, which significantly impacts ice dynamics in regions such as High Mountain Asia (Rounce et al., 2020). Further, even a single glacier model may produce a large spread in certain runoff metrics — comparable to inter-GCM spread — when subjected to different choices of historical climate dataset and initial glacier geometry (Aguayo et al., 2024). Downstream users must therefore carefully define their requirements, and consult the glacier model description literature, to ensure an appropriate choice of glacier model and initialization datasets.

## 5 Conclusions

We have used all suitable global glacier models, forced by an ensemble of the most up-to-date global climate models, to quantify glacial drought buffering on the Standardized Precipitation-Evapotranspiration Index. Glacial drought buffering correlates with basin glacier coverage, and buffering generally increases or stays steady through the end of the 21st century. The consistency of this result with Ultee et al. (2022) indicates that it is robust to choice of glacier model, choice of CMIP5 or CMIP6 forcing, and choice of baseline period. Our results should reassure glacier modellers that large inter-glacier-model differences in some output variables do not hinder their utility for downstream impact studies. By contrast, the spread resulting from the climate model forcing is greater than that from different glacier models, even though we have not fully sampled the sources of climate model uncertainty. Future downstream hydrological studies that wish to use glacier model output can justify using only one of the available glacier models, if well chosen for their regional context. However, it is imperative that downstream hydrological studies and the next generation of global glacier model projections select and analyse a representative ensemble of climate model simulations for climate forcing.

*Code and data availability.* The glacier model runoff aggregated to basin scale is archived as Wimberly (2024). The OGGM standard runoff projections are a variant of Schuster et al. (2023b). The PyGEM runoff projections are archived as Rounce et al. (2022). The code for our analysis is available on GitHub and archived on Zenodo (DOI: 10.5281/zenodo.6510185).



## 250 Appendix A: Regional maps

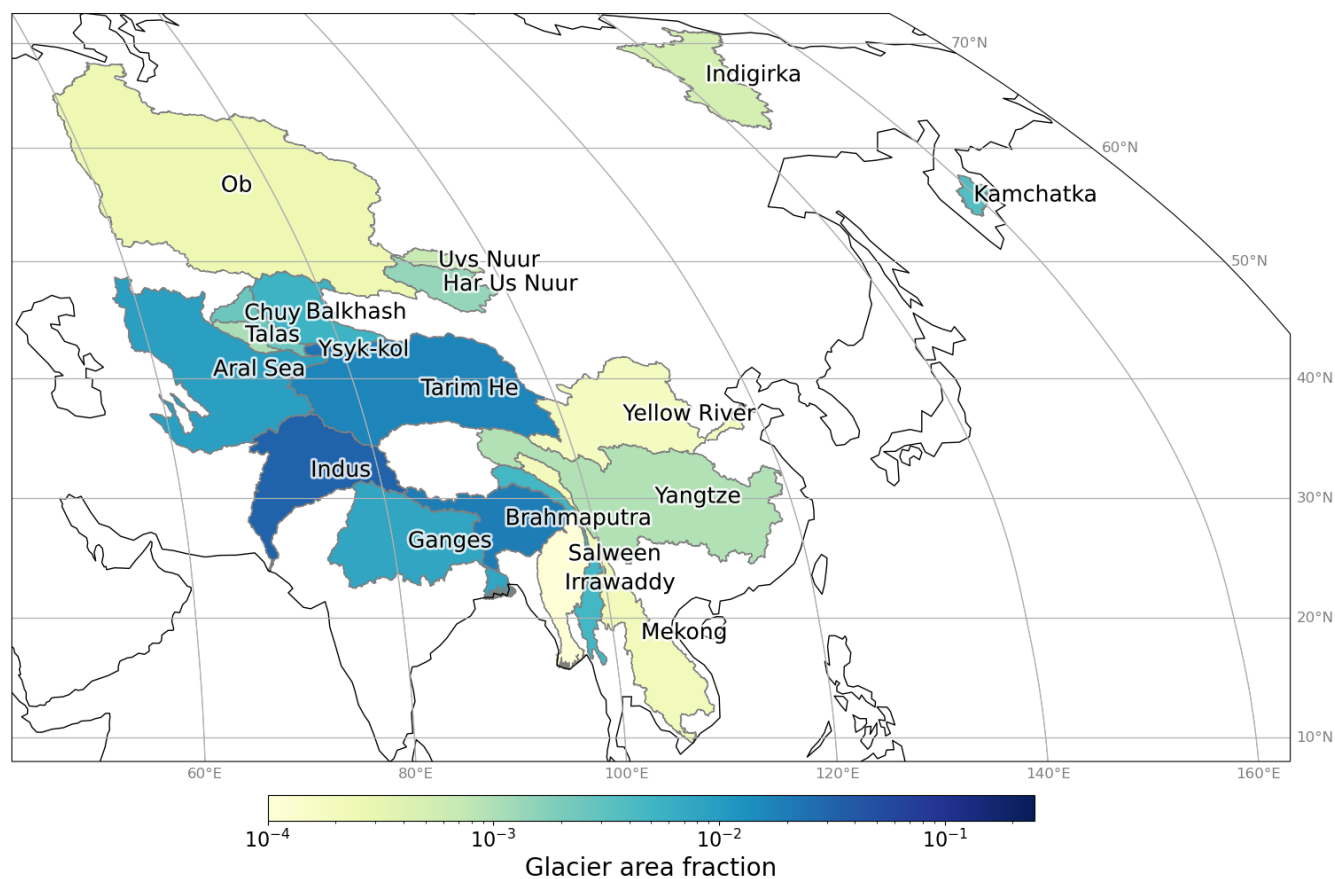


**Figure A1.** River basins of Asia included in this study, colored by the glacier area fraction  $A_g/A_{basin}$ .

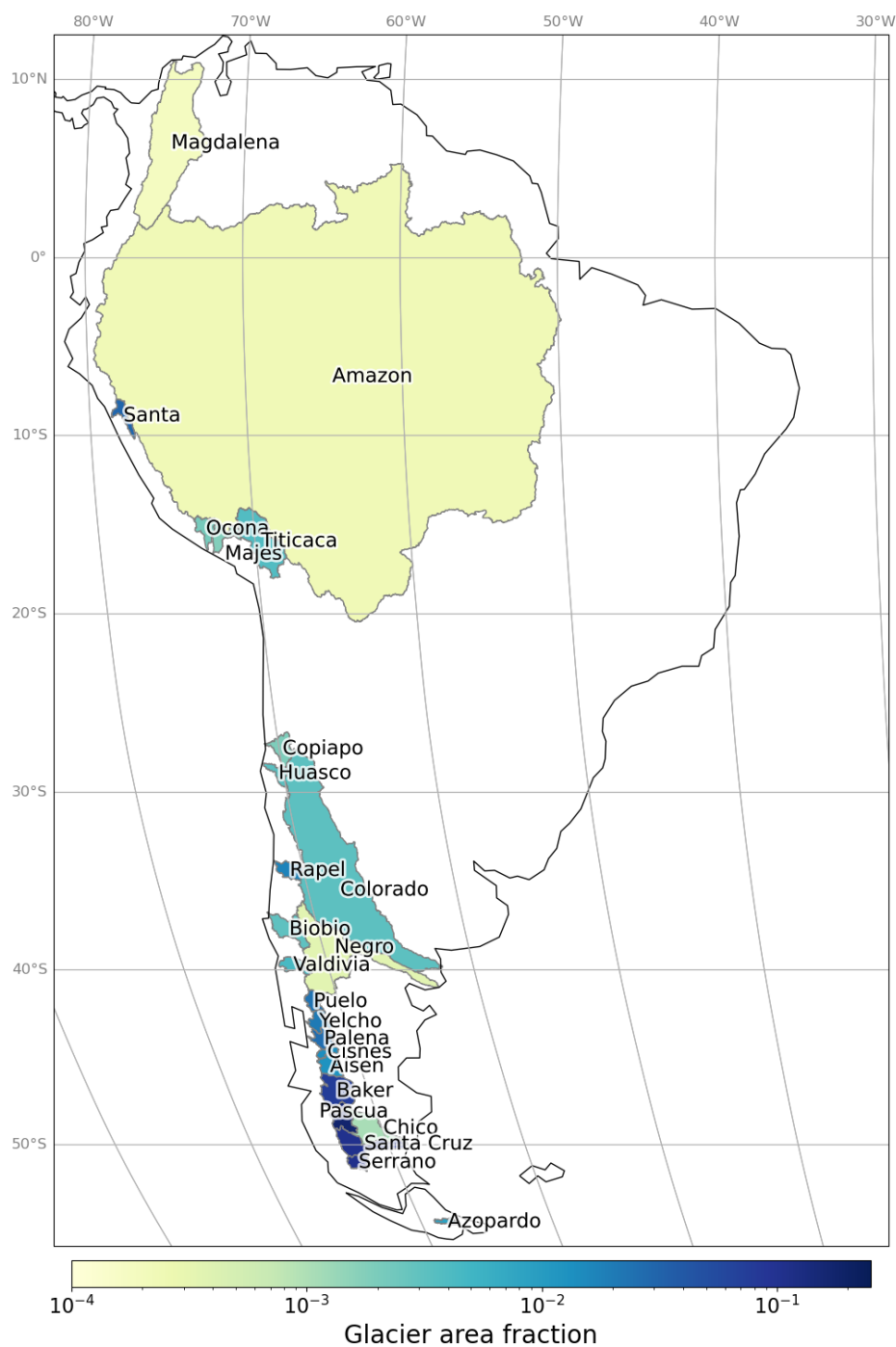


**Figure A2.** River basins of South America included in this study, colored by the glacier area fraction  $A_g/A_{basin}$ .



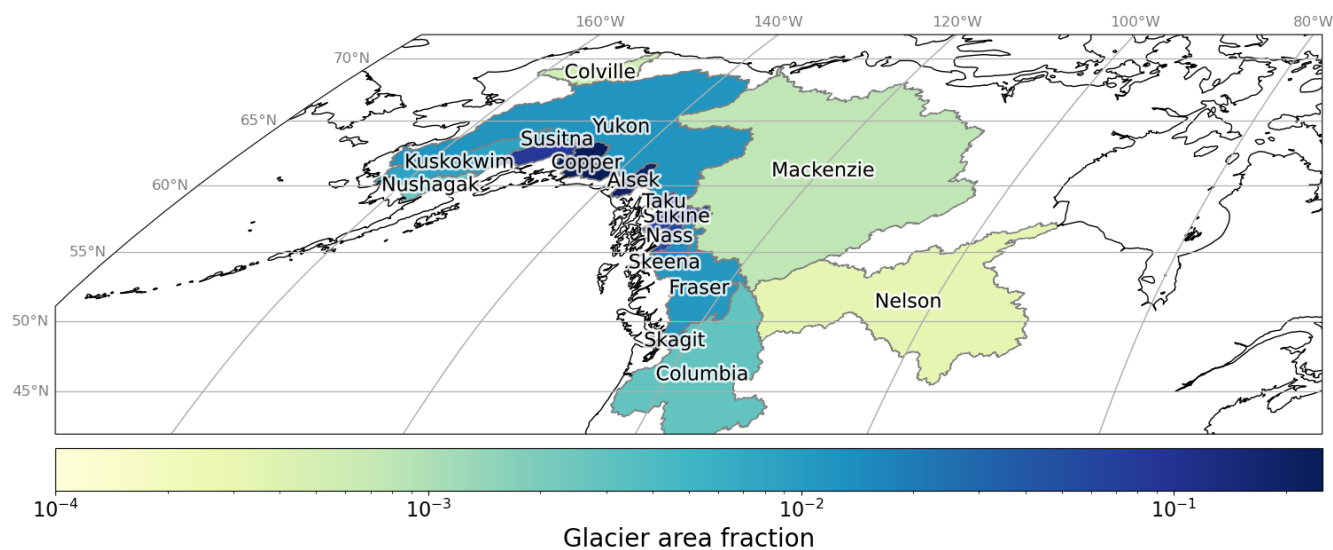


**Figure A3.** River basins of North America included in this study, colored by the glacier area fraction  $A_g/A_{basin}$ .

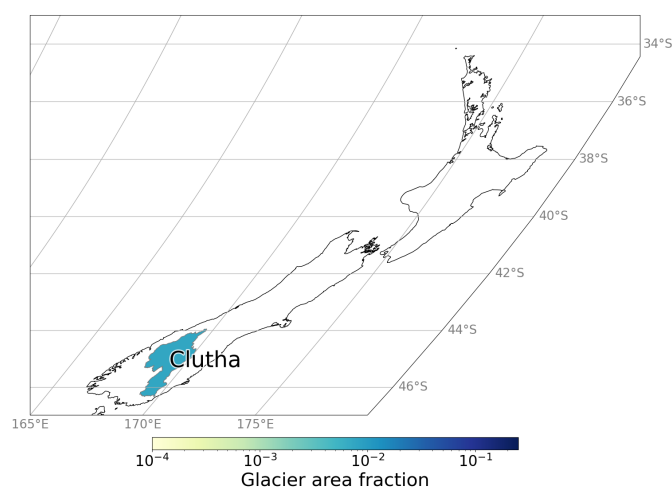


**Figure A4.** The single New Zealand river basin included in this study, colored by the glacier area fraction  $A_g/A_{basin}$ .

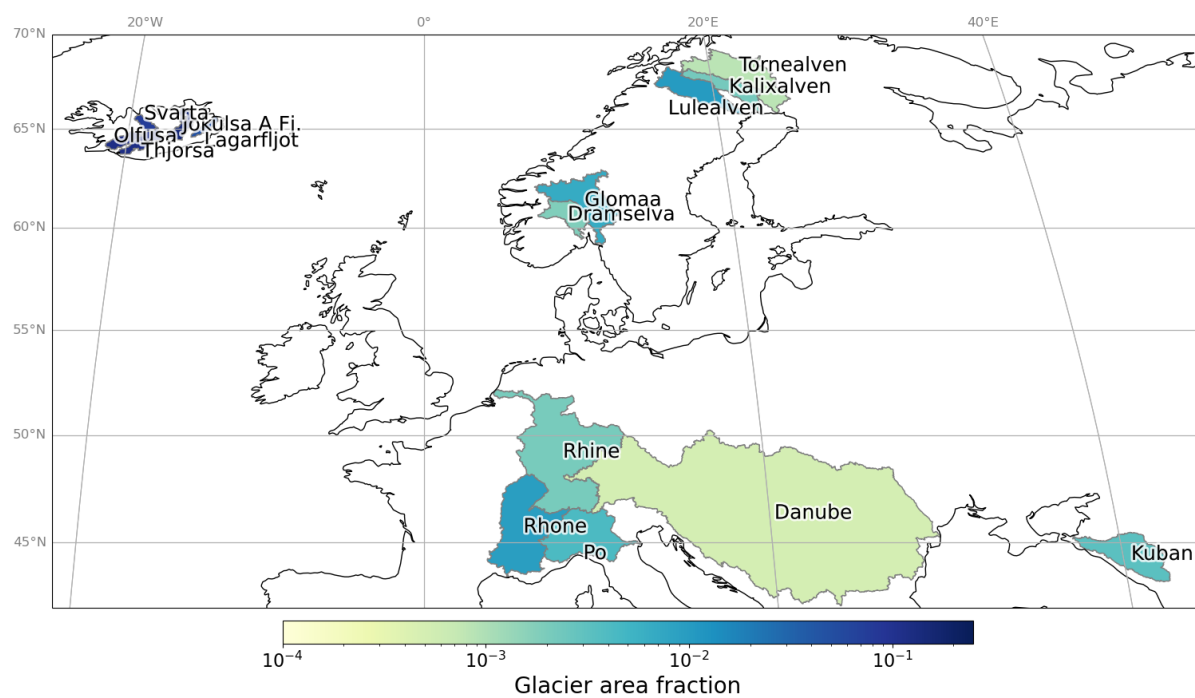


**Figure A5.** River basins of Europe included in this study, colored by the glacier area fraction  $A_g/A_{basin}$ .



## Appendix B: Per-basin comparison with CMIP6 archive

*Author contributions.* LU conceived of the study. SC and JM consulted on methodology. FW and EH conducted related analyses that informed the methods. FW aggregated and processed all glacier model data. SC aggregated global climate model data and computed SPEI values. LU and FW made figures. LU drafted the manuscript, and all authors edited and approved its final form.

255 *Competing interests.* The authors declare that no competing interests are present.

*Acknowledgements.* The authors thank the developer teams of the glacier models GloGEM, PyGEM, and OGGM for their efforts in providing runoff outputs and discussing interpretation. Lilian Schuster completed and archived the public OGGM simulations studied here. Brandon Tober completed the PyGEM simulations; Matthias Huss completed the GloGEM simulations. JM's contribution was funded by the Natural Environment Research Council (NERC) MCNC Grant TerraFirma NE/W004895/1.

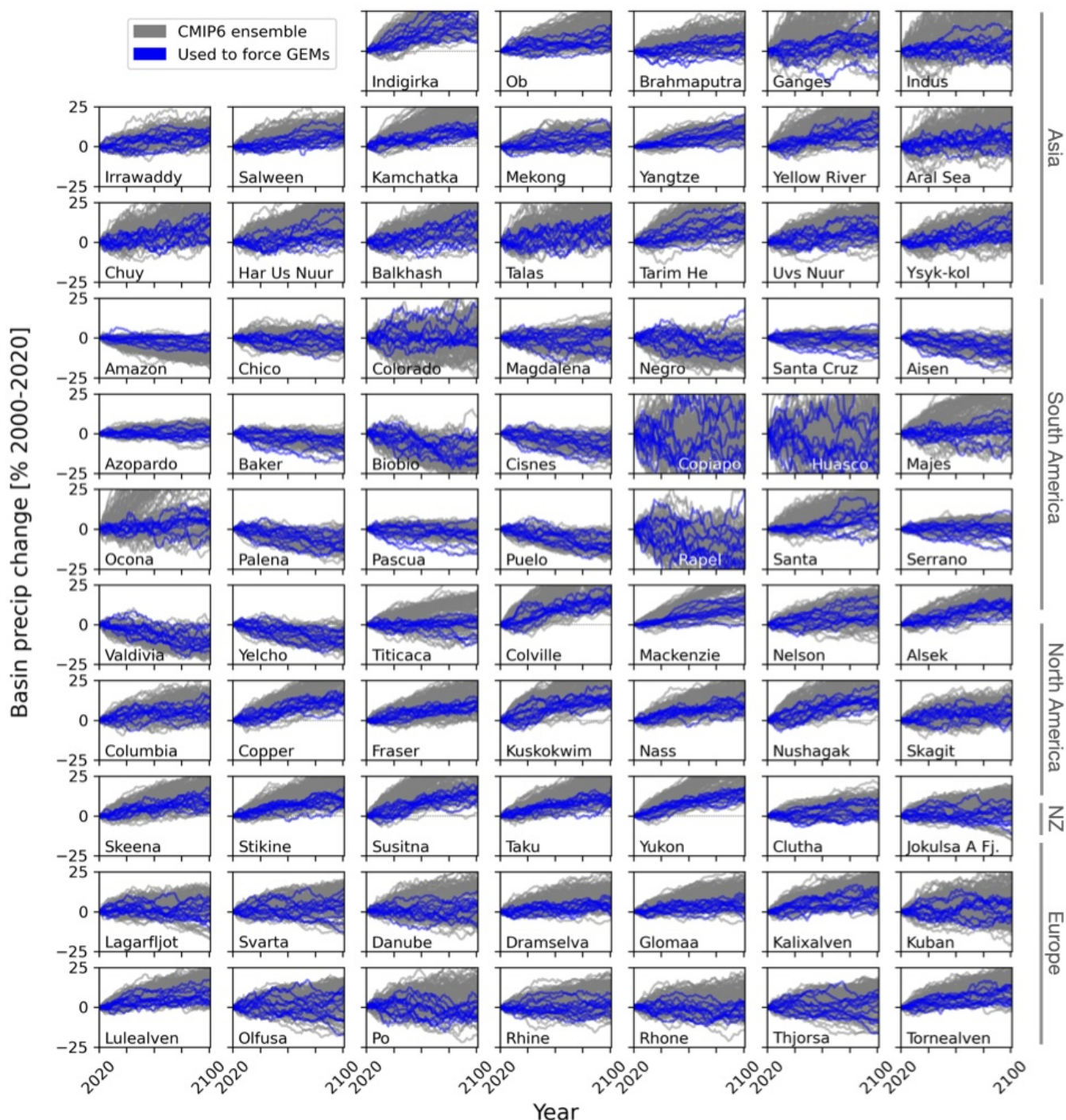


**Figure B1.** Change in precipitation over the 21st century, forced by SSP2-4.5, for an ensemble of 112 CMIP6 simulations (grey lines) compared with the 11-member ensemble used to force the glacier models (blue lines). Changes are expressed as percent change with respect to a 2000-2020 baseline.



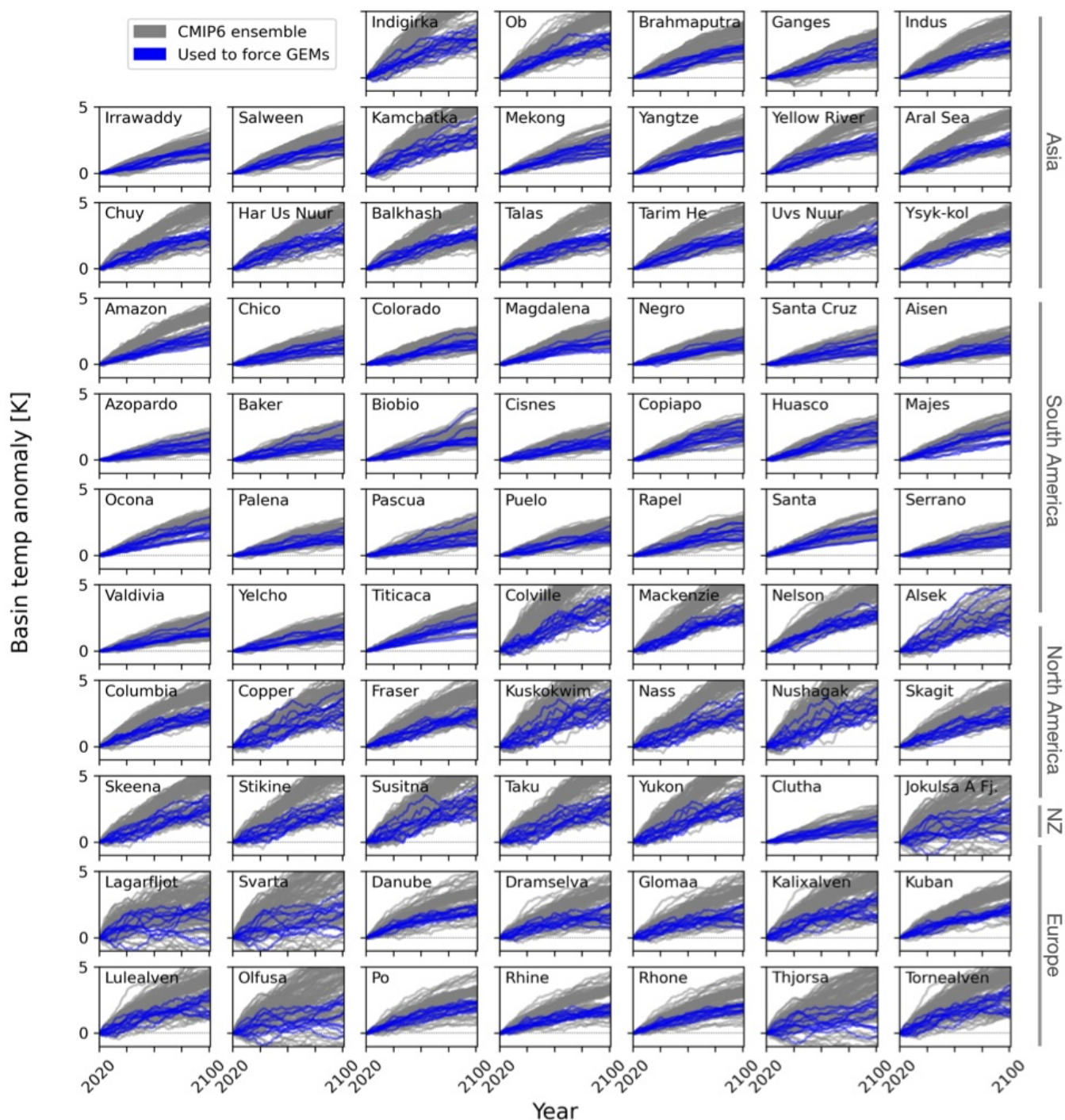


**Figure B2.** Change in temperature over the 21st century, forced by SSP2-4.5, for an ensemble of 112 CMIP6 simulations (grey lines) compared with the 11-member ensemble used to force the glacier models (blue lines). Changes are temperature anomaly (K) from a 2000-2020 baseline.



## 260 References

- Aguayo, R., Maussion, F., Schuster, L., Schaefer, M., Caro, A., Schmitt, P., Mackay, J., Ultee, L., Leon-Muñoz, J., and Aguayo, M.: Unravelling the sources of uncertainty in glacier runoff projections in the Patagonian Andes (40–56° S), *The Cryosphere*, 18, 5383–5406, <https://doi.org/10.5194/tc-18-5383-2024>, 2024.
- Caretta, M. A., Mukherji, A., Arfanuzzaman, M., Betts, R. A., Gelfan, A., Hirabayashi, Y., Lissner, T. K., Liu, J., Gunn, E. L., Morgan, R.,  
265 Mwanga, S., and Supratid, S.: Water, in: *Climate Change 2022: Impacts, Adaptation and Vulnerability. Contribution of Working Group II to the Sixth Assessment Report of the Intergovernmental Panel on Climate Change*, edited by Pörtner, H.-O., Roberts, D., Tignor, M., Poloczanska, E., Mintenbeck, K., Alegría, A., Craig, M., Langsdorf, S., Löschke, S., Möller, V., Okem, A., and Rama, B., pp. 551–712, Cambridge University Press, Cambridge, UK and New York, NY, USA, <https://doi.org/doi:10.1017/9781009325844.006>, 2022.
- Chen, J. and Ohmura, A.: On the influence of Alpine glaciers on runoff, *IAHS Publ*, 193, 117–125, 1990.
- 270 Compagno, L., Huss, M., Miles, E. S., McCarthy, M. J., Zekollari, H., Dehecq, A., Pellicciotti, F., and Farinotti, D.: Modelling supraglacial debris-cover evolution from the single-glacier to the regional scale: an application to High Mountain Asia, *The Cryosphere*, 16, 1697–1718, <https://doi.org/10.5194/tc-16-1697-2022>, 2022.
- Cook, B. I., Mankin, J. S., Marvel, K., Williams, A. P., Smerdon, J. E., and Anchukaitis, K. J.: Twenty-first century drought projections in the CMIP6 forcing scenarios, *Earth’s Future*, p. e2019EF001461, <https://doi.org/10.1029/2019EF001461>, 2020.
- 275 Danandeh Mehr, A. and Vaheddoost, B.: Identification of the trends associated with the SPI and SPEI indices across Ankara, Turkey, *Theoretical and Applied Climatology*, 139, 1531–1542, <https://doi.org/https://doi.org/10.1007/s00704-019-03071-9>, 2020.
- Decharme, B., Delire, C., Minvielle, M., Colin, J., Vergnes, J.-P., Alias, A., Saint-Martin, D., Séférian, R., Sénézi, S., and Voldoire, A.: Recent changes in the ISBA-CTRIP land surface system for use in the CNRM-CM6 climate model and in global off-line hydrological applications, *Journal of Advances in Modeling Earth Systems*, 11, 1207–1252, <https://doi.org/10.1029/2018MS001545>, 2019.
- 280 Deser, C., Lehner, F., Rodgers, K. B., Ault, T., Delworth, T. L., DiNezio, P. N., Fiore, A., Frankignoul, C., Fyfe, J. C., Horton, D. E., Kay, J. E., Knutti, R., Lovenduski, N. S., Marotzke, J., McKinnon, K. A., Minobe, S., Randerson, J., Screen, J. A., Simpson, I. R., and Ting, M.: Insights from Earth system model initial-condition large ensembles and future prospects, *Nature Climate Change*, 10, 277–286, <https://doi.org/10.1038/s41558-020-0731-2>, 2020.
- Douville, H., Raghavan, K., Renwick, J., Allan, R. P., Arias, P. A., Barlow, M., Cerezo-Mota, R., Cherchi, A., Gan, T. Y., Gergis, J., Jiang,  
285 D., Khan, A., Mba, W. P., Rosenfeld, D., Tierney, J., and Zolina, O.: Water cycle changes, in: *Climate Change 2021: The Physical Science Basis. Contribution of Working Group I to the Sixth Assessment Report of the Intergovernmental Panel on Climate Change*, edited by Masson-Delmotte, V. P., Zhai, P., Pirani, A., Connors, S. L., Péan, C., Berger, S., Caud, N., Chen, Y., Goldfarb, L., Gomis, M. I., Huang, M., Leitzell, K., Lonno, E., Matthews, J. B. R., Maycock, T. K., Waterfield, T., Yelekçi, O., Yu, R., and Zhou, B., pp. 1055–1210, Cambridge University Press, Cambridge, UK, <https://doi.org/10.1017/9781009157896.010>, 2021.
- 290 Eyring, V., Bony, S., Meehl, G. A., Senior, C. A., Stevens, B., Stouffer, R. J., and Taylor, K. E.: Overview of the Coupled Model Intercomparison Project Phase 6 (CMIP6) experimental design and organization, *Geoscientific Model Development*, 9, 1937–1958, <https://doi.org/10.5194/gmd-9-1937-2016>, 2016.
- Farahmand, A. and AghaKouchak, A.: A generalized framework for deriving nonparametric standardized drought indicators, *Advances in Water Resources*, 76, 140–145, <https://doi.org/10.1016/j.advwatres.2014.11.012>, 2015.
- 295 Fleming, S. W. and Clarke, G. K.: Attenuation of High-Frequency Interannual Streamflow Variability by Watershed Glacial Cover, *Journal of Hydraulic Engineering*, 131, 615–618, [https://doi.org/10.1061/\(ASCE\)0733-9429\(2005\)131:7\(615\)](https://doi.org/10.1061/(ASCE)0733-9429(2005)131:7(615)), 2005.





- Global Runoff Data Centre: GRDC Major River Basins, <http://grdc.bafg.de>, [https://grdc.bafg.de/GRDC/EN/02\\_srvcs/22\\_gslrs/221\\_MRB/riverbasins\\_node.html](https://grdc.bafg.de/GRDC/EN/02_srvcs/22_gslrs/221_MRB/riverbasins_node.html), 2020.
- Hanus, S., Schuster, L., Burek, P., Maussion, F., Wada, Y., and Viviroli, D.: Coupling a large-scale glacier and hydrological model (OGGM v1.5.3 and CWatM V1.08) – towards an improved representation of mountain water resources in global assessments, *Geoscientific Model Development*, 17, 5123–5144, <https://doi.org/10.5194/gmd-17-5123-2024>, 2024.
- Hock, R., Bliss, A., Marzeion, B., Giesen, R. H., Hirabayashi, Y., Huss, M., Radić, V., and Slangen, A. B.: GlacierMIP –A model intercomparison of global-scale glacier mass-balance models and projections, *Journal of Glaciology*, 65, 453–467, <https://doi.org/DOI:10.1017/jog.2019.22>, 2019.
- Huss, M. and Hock, R.: A new model for global glacier change and sea-level rise, *Frontiers in Earth Science*, 3, <https://doi.org/10.3389/feart.2015.00054>, 2015.
- Huss, M. and Hock, R.: Global-scale hydrological response to future glacier mass loss, *Nature Climate Change*, 8, 135–140, <https://doi.org/10.1038/s41558-017-0049-x>, 2018.
- Immerzeel, W. W., Lutz, A. F., Andrade, M., Bahl, A., Biemans, H., Bolch, T., Hyde, S., Brumby, S., Davies, B. J., Elmore, A. C., Emmer, A., Feng, M., Fernández, A., Haritashya, U., Kargel, J. S., Koppes, M., Kraaijenbrink, P. D. A., Kulkarni, A. V., Mayewski, P. A., Nepal, S., Pacheco, P., Painter, T. H., Pellicciotti, F., Rajaram, H., Rupper, S., Sinisalo, A., Shrestha, A. B., Viviroli, D., Wada, Y., Xiao, C., Yao, T., and Baillie, J. E. M.: Importance and vulnerability of the world’s water towers, *Nature*, 577, 364–369, <https://doi.org/10.1038/s41586-019-1822-y>, 2020.
- Kumar, A., Gosling, S. N., Johnson, M. F., Jones, M. D., Zaherpour, J., Kumar, R., Leng, G., Schmied, H. M., Kupzig, J., Breuer, L., Hanasaki, N., Tang, Q., Ostberg, S., Stacke, T., Pokhrel, Y., Wada, Y., and Masaki, Y.: Multi-model evaluation of catchment- and global-scale hydrological model simulations of drought characteristics across eight large river catchments, *Advances in Water Resources*, 165, 104212, <https://doi.org/https://doi.org/10.1016/j.advwatres.2022.104212>, 2022.
- Lawrence, D. M., Fisher, R. A., Koven, C. D., Oleson, K. W., Swenson, S. C., Bonan, G., Collier, N., Ghimire, B., van Kampenhout, L., Kennedy, D., Kluzek, E., Lawrence, P. J., Li, F., Li, H., Lombardozzi, D., Riley, W. J., Sacks, W. J., Shi, M., Vertenstein, M., Wieder, W. R., Xu, C., Ali, A. A., Badger, A. M., Bisht, G., van den Broeke, M., Brunke, M. A., Burns, S. P., Buzan, J., Clark, M., Craig, A., Dahlin, K., Drewniak, B., Fisher, J. B., Flanner, M., Fox, A. M., Gentine, P., Hoffman, F., Keppel-Aleks, G., Knox, R., Kumar, S., Lenaerts, J., Leung, L. R., Lipscomb, W. H., Lu, Y., Pandey, A., Pelletier, J. D., Perket, J., Randerson, J. T., Ricciuto, D. M., Sanderson, B. M., Slater, A., Subin, Z. M., Tang, J., Thomas, R. Q., Val Martin, M., and Zeng, X.: The Community Land Model Version 5: Description of New Features, Benchmarking, and Impact of Forcing Uncertainty, *Journal of Advances in Modeling Earth Systems*, 11, 4245–4287, <https://doi.org/https://doi.org/10.1029/2018MS001583>, 2019.
- López-Moreno, J., Vicente-Serrano, S., Zabalza, J., Beguería, S., Lorenzo-Lacruz, J., Azorin-Molina, C., and Morán-Tejeda, E.: Hydrological response to climate variability at different time scales: A study in the Ebro basin, *Journal of Hydrology*, 477, 175–188, <https://doi.org/https://doi.org/10.1016/j.jhydrol.2012.11.028>, 2013.
- Mackay, J. D., Barrand, N. E., Hannah, D. M., Krause, S., Jackson, C. R., Everest, J., and Aðalgeirsdóttir, G.: Glacio-hydrological melt and run-off modelling: application of a limits of acceptability framework for model comparison and selection, *The Cryosphere*, 12, 2175–2210, <https://doi.org/10.5194/tc-12-2175-2018>, 2018.
- Mackay, J. D., Barrand, N. E., Hannah, D. M., Krause, S., Jackson, C. R., Everest, J., Aðalgeirsdóttir, G., and Black, A. R.: Future evolution and uncertainty of river flow regime change in a deglaciating river basin, *Hydrology and Earth System Sciences*, 23, 1833–1865, <https://doi.org/10.5194/hess-23-1833-2019>, 2019.



- 335 Marzeion, B., Hock, R., Anderson, B., Bliss, A., Champollion, N., Fujita, K., Huss, M., Immerzeel, W., Kraaijenbrink, P., Malles, J.-H.,  
 Maussion, F., Radić, V., Rounce, D. R., Sakai, A., Shannon, S., van de Wal, R., and Zekollari, H.: Partitioning the Uncertainty of Ensemble  
 Projections of Global Glacier Mass Change, *Earth's Future*, p. e2019EF001470, <https://doi.org/10.1029/2019EF001470>, 2020.
- Maussion, F., Butenko, A., Champollion, N., Dusch, M., Eis, J., Fourteau, K., Gregor, P., Jarosch, A. H., Landmann, J., Oesterle, F., Recinos,  
 B., Rothenpieler, T., Vlug, A., Wild, C. T., and Marzeion, B.: The Open Global Glacier Model (OGGM) v1.1, *Geoscientific Model*  
 340 *Development*, 12, 909–931, <https://doi.org/10.5194/gmd-12-909-2019>, 2019.
- Maussion, F., Rothenpieler, T., Dusch, M., Schmitt, P., Vlug, A., Schuster, L., Champollion, N., Li, F., Marzeion, B., Oberrauch, M., Eis,  
 J., Fischer, A., Landmann, J., Jarosch, A., luzpaz, Hanus, S., Rounce, D., Castellani, M., Bartholomew, S. L., Minallah, S., bowen-  
 belongstonature, Merrill, C., Otto, D., Loibl, D., Rosa, G., Ultee, L., Thompson, S., anton ub, and Gregor, P.: OGGM/oggm: v1.6.1,  
<https://doi.org/10.5281/zenodo.8287580>, 2023.
- 345 Naz, B. S., Frans, C. D., Clarke, G. K. C., Burns, P., and Lettenmaier, D. P.: Modeling the effect of glacier recession on streamflow response  
 using a coupled glacio-hydrological model, *Hydrology and Earth System Sciences*, 18, 787–802, [https://doi.org/10.5194/hess-18-787-](https://doi.org/10.5194/hess-18-787-2014)  
 2014, 2014.
- O'Loughlin, R.: Why we need lower-performance climate models, *Climatic Change*, 177, [https://doi.org/https://doi.org/10.1007/s10584-](https://doi.org/https://doi.org/10.1007/s10584-023-03661-7)  
 023-03661-7, 2024.
- 350 Pesci, M. H., Schulte Overberg, P., Bosshard, T., and Förster, K.: From global glacier modeling to catchment hydrology: bridging the gap  
 with the WaSiM-OGGM coupling scheme, *Frontiers in Water*, 5, <https://doi.org/10.3389/frwa.2023.1296344>, 2023.
- Prudhomme, C., Giuntoli, I., Robinson, E. L., Clark, D. B., Arnell, N. W., Dankers, R., Fekete, B. M., Franssen, W., Gerten, D., Gosling,  
 S. N., Hagemann, S., Hannah, D. M., Kim, H., Masaki, Y., Satoh, Y., Stacke, T., Wada, Y., and Wisser, D.: Hydrological droughts in  
 the 21st century, hotspots and uncertainties from a global multimodel ensemble experiment, *Proceedings of the National Academy of*  
 355 *Sciences*, 111, 3262–3267, <https://doi.org/10.1073/pnas.1222473110>, 2014.
- RGI Consortium: Randolph Glacier Inventory – A Dataset of Global Glacier Outlines: Version 6.0, Technical Report, Global Land Ice  
 Measurements from Space, 2017.
- Rounce, D. R., Hock, R., and Shean, D. E.: Glacier Mass Change in High Mountain Asia Through 2100 Using the Open-Source Python  
 Glacier Evolution Model (PyGEM), *Frontiers in Earth Science*, 7, 331, <https://doi.org/10.3389/feart.2019.00331>, 2020.
- 360 Rounce, D. R., Hock, R., and Maussion, F.: Global PyGEM-OGGM Glacier Projections with RCP and SSP Scenarios, Version 1,  
<https://doi.org/10.5067/P8BN9VO9N5C7>, 2022.
- Rounce, D. R., Hock, R., Maussion, F., Hugonnet, R., Kochtitzky, W., Huss, M., Berthier, E., Brinkerhoff, D., Compagno, L., Copland,  
 L., Farinotti, D., Menounos, B., and McNabb, R. W.: Global glacier change in the 21st century: Every increase in temperature matters,  
*Science*, 379, 78–83, <https://doi.org/10.1126/science.abo1324>, 2023.
- 365 Salzmann, N., Huggel, C., Rohrer, M., and Stoffel, M.: Data and knowledge gaps in glacier, snow and related runoff research – A climate  
 change adaptation perspective, *Journal of Hydrology*, 518, 225–234, <https://doi.org/https://doi.org/10.1016/j.jhydrol.2014.05.058>, climatic  
 change impact on water: Overcoming data and science gaps, 2014.
- Satoh, Y., Shiogama, H., Hanasaki, N., Pokhrel, Y., Boulange, J. E. S., Burek, P., Gosling, S. N., Grillakis, M., Koutroulis, A., Schmied,  
 H. M., Thiery, W., and Yokohata, T.: A quantitative evaluation of the issue of drought definition: a source of disagreement in future  
 370 drought assessments, *Environmental Research Letters*, 16, 104 001, <https://doi.org/10.1088/1748-9326/ac2348>, 2021.
- Scheff, J., Coats, S., and Laguë, M. M.: Why do the Global Warming Responses of Land-Surface Models and Climatic Dryness Metrics  
 Disagree?, *Earth's Future*, 10, e2022EF002 814, <https://doi.org/https://doi.org/10.1029/2022EF002814>, 2022.



- Schuster, L., Rounce, D. R., and Maussion, F.: Glacier projections sensitivity to temperature-index model choices and calibration strategies, *Annals of Glaciology*, pp. 1–16, <https://doi.org/DOI: 10.1017/aog.2023.57>, 2023a.
- 375 Schuster, L., Schmitt, P., Vlug, A., and Maussion, F.: OGGM/oggm-standard-projections-csv-files: v1.0 (v1.0), Zenodo, <https://doi.org/https://doi.org/10.5281/zenodo.8286065>, 2023b.
- Schuster, L., Maussion, F., Rounce, D. R., Ultee, L., Schmitt, P., Lacroix, F., Frölicher, T. L., and Schleussner, C.-F.: Irreversible glacier change and trough water for centuries after overshooting 1.5 °C, *Nature Climate Change*, 15, 634–641, <https://doi.org/10.1038/s41558-025-02318-w>, 2025.
- 380 Somers, L. D. and McKenzie, J. M.: A review of groundwater in high mountain environments, *WIREs Water*, 7, e1475, <https://doi.org/https://doi.org/10.1002/wat2.1475>, 2020.
- Stein, L., Mukkavilli, S. K., Pfitzmann, B. M., Staar, P. W. J., Ozturk, U., Berrospi, C., Brunschweiler, T., and Wagener, T.: Wealth Over Woe: Global Biases in Hydro-Hazard Research, *Earth's Future*, 12, e2024EF004 590, <https://doi.org/https://doi.org/10.1029/2024EF004590>, 2024.
- 385 Ultee, L., Coats, S., and Mackay, J.: Glacial runoff buffers droughts through the 21st century, *Earth System Dynamics*, 13, 935–959, <https://doi.org/10.5194/esd-13-935-2022>, 2022.
- Van Loon, A. F., Stahl, K., Di Baldassarre, G., Clark, J., Rangecroft, S., Wanders, N., Gleeson, T., Van Dijk, A. I. J. M., Tallaksen, L. M., Hannaford, J., Uijlenhoet, R., Teuling, A. J., Hannah, D. M., Sheffield, J., Svoboda, M., Verbeiren, B., Wagener, T., and Van Lanen, H. A. J.: Drought in a human-modified world: reframing drought definitions, understanding, and analysis approaches, *Hydrology and Earth*
- 390 *System Sciences*, 20, 3631–3650, <https://doi.org/10.5194/hess-20-3631-2016>, 2016.
- van Tiel, M., Kohn, I., Van Loon, A. F., and Stahl, K.: The compensating effect of glaciers: Characterizing the relation between interannual streamflow variability and glacier cover, *Hydrological Processes*, 34, 553–568, <https://doi.org/10.1002/hyp.13603>, 2020a.
- van Tiel, M., Stahl, K., Freudiger, D., and Seibert, J.: Glacio-hydrological model calibration and evaluation, *WIREs Water*, 7, e1483, <https://doi.org/https://doi.org/10.1002/wat2.1483>, 2020b.
- 395 Wanders, N., Wada, Y., and Van Lanen, H. A. J.: Global hydrological droughts in the 21st century under a changing hydrological regime, *Earth System Dynamics*, 6, 1–15, <https://doi.org/10.5194/esd-6-1-2015>, 2015.
- Wiersma, P., Aerts, J., Zekollari, H., Hrachowitz, M., Drost, N., Huss, M., Sutanudjaja, E. H., and Hut, R.: Coupling a global glacier model to a global hydrological model prevents underestimation of glacier runoff, *Hydrology and Earth System Sciences*, 26, 5971–5986, <https://doi.org/10.5194/hess-26-5971-2022>, 2022.
- 400 Wimberly, F.: Processed Runoff Files, Data Dryad, 2024.
- Wimberly, F., Ultee, L., Schuster, L., Huss, M., Rounce, D. R., Maussion, F., Coats, S., Mackay, J., and Holmgren, E.: Inter-model differences in 21st century glacier runoff for the world's major river basins, *The Cryosphere*, 19, 1491–1511, <https://doi.org/10.5194/tc-19-1491-2025>, 2025.
- Yang, Y., Roderick, M. L., Zhang, S., McVicar, T. R., and Donohue, R. J.: Hydrologic implications of vegetation response to elevated CO<sub>2</sub> in climate projections, *Nature Climate Change*, 9, 44, <https://doi.org/10.1038/s41558-018-0361-0>, 2019.
- 405 Zekollari, H., Huss, M., Schuster, L., Maussion, F., Rounce, D. R., Aguayo, R., Champollion, N., Compagno, L., Hugonnet, R., Marzeion, B., Mojtavavi, S., and Farinotti, D.: Twenty-first century global glacier evolution under CMIP6 scenarios and the role of glacier-specific observations, *The Cryosphere*, 18, 5045–5066, <https://doi.org/10.5194/tc-18-5045-2024>, 2024.